ESAIM: M2AN 46 (2012) 1407–1420
DOI: 10.1051/m2an/2012004

ESAIM: Mathematical Modelling and Numerical Analysis
www.esaim-m2an.org

EFFICIENT COMPUTATION OF DELAY DIFFERENTIAL EQUATIONS WITH HIGHLY OSCILLATORY TERMS

Marissa Condon[1], Alfredo Deaño[2], Arieh Iserles[3] and Karolina Kropielnicka[3,4]

Abstract. This paper is concerned with the asymptotic expansion and numerical solution of systems of linear delay differential equations with highly oscillatory forcing terms. The computation of such problems using standard numerical methods is exceedingly slow and inefficient, indeed standard software is practically useless for this purpose. We propose an alternative, consisting of an asymptotic expansion of the solution, where each term can be derived either by recursion or by solving a non-oscillatory problem. This leads to methods which, counter-intuitively to those developed according to standard numerical reasoning, exhibit improved performance with growing frequency of oscillation.

Mathematics Subject Classification. 34E05, 34E99, 42A99, 34K28.

Received March 18, 2011. Revised December 15, 2011.
Published online April 19, 2012.

1. Introduction

There is a growing interest in the numerical solution of differential equations with high oscillatory solutions, motivated in large measure by their very wide range of applications in mathematical modelling [8]. Such equations come in two basic 'flavours': the oscillation can originate either in intrinsic features of the underlying differential problem [5] or in the presence of a highly oscillatory forcing term [2, 7].

A rich source of highly oscillatory problems with extrinsic oscillation (*i.e.*, when the oscillation originates in a forcing term) is computational electronic engineering. The eternal quest for accurate models has led to an increasing interest in delay differential equations for engineering applications. Delays arise whenever signals are transmitted over a finite distance from one point to another, so accurate models of communication systems inevitably should include delay differential equations. In their paper Kyrychko and Hogan [9] provide a vast array of applications of delay differential equations in engineering. Some applications worth highlighting include laser dynamics [11] and the related secure communication techniques using chaos [10]. Analysis of coupled microwave oscillators also requires the inclusion of delays as frequencies are above 10 GHz in such systems [12], consequently

Keywords and phrases. Delay differential equations, asymptotic expansions, modulated Fourier expansions, numerical analysis.

[1] School of Electronic Engineering, Dublin City University, Dublin 9, Ireland. marissa.condon@dcu.ie

[2] Dpto. de Matemáticas, Universidad Carlos III de Madrid, Avda. Universidad, 30, Leganés 28911, Madrid, Spain

[3] Department of Applied Mathematics and Theoretical Physics, Centre for Mathematical Sciences, University of Cambridge, Wilberforce Rd, CB3 0WA Cambridge, UK

[4] Institute of Mathematics, University of Gdańsk, Wit Stwosz Str. 57, 80-952 Gdańsk, Poland

Article published by EDP Sciences

the time for light to travel the typically few centimetres between the oscillators is significant. Chembo *et al.* [4] specifically mention the difficulties in relation to numerical analysis of optoelectronic microwave oscillators. These state of the art microwave generators are increasingly of interest in the area of high-precision radar and sensor technology and accurate efficient numerical simulation is crucial for efficient engineering design.

The modelling of highly oscillatory electronic circuits results in ordinary, partial, differential-algebraic and delay differential problems. While our understanding of ordinary differential equations with extrinsic oscillation has advanced greatly following recent research and effective numerical methods are available [3,6], the solution of delay differential equations with highly oscillatory forcing terms is largely unexplored. This paper is devoted to an initial foray into this subject matter and concerns itself with the asymptotic and numerical solution of linear systems of this kind.

More specifically, we are concerned with a system of linear delay differential equations (DDEs) of the form

$$\boldsymbol{y}'(t) = A\boldsymbol{y}(t) + B\boldsymbol{y}(t-1) + \sum_{m=-\infty}^{\infty} \boldsymbol{a}_m(t)\mathrm{e}^{\mathrm{i}m\omega t}, \qquad 0 \le t \le T, \tag{1.1}$$

with the initial condition

$$\boldsymbol{y}(t) = \boldsymbol{\varphi}(t), \qquad -1 \le t < 0, \tag{1.2}$$

where $\boldsymbol{y}(t),\ \boldsymbol{a}_m(t) : \mathbb{C} \to \mathbb{C}^d,\ m \in \mathbb{Z}$, while A and B are $d \times d$ constant matrices. In particular, we are interested in the case when $\omega \gg 1$. Note that the forcing term, the origin of rapid oscillations is written in a form of a *modulated Fourier expansion* (MFE). Such expansions have been pioneered by Cohen *et al.* [5] in backward error analysis of partial differential equations, subsequently used by Sanz-Serna and his collaborators in their work on the heterogeneous multiscale method [2,3], as well as in our research into different types of extrinsic high oscillations [6,7].

Standard forcing terms, *e.g.* $\boldsymbol{a}\sin\omega t$, are an obvious special case of an MFE, as are 'plain' Fourier series. However, the extra generality afforded by MFE comes at no extra price and, even were we to commence with $\boldsymbol{a}\sin\omega t$, say, MFEs would have anyway appeared in our expansions. Therefore, we may just as well commence from this more general setting.

There exist numerous methods for the numerical solution of delay differential equations, mostly based upon an extension of key tools in the numerical analysis of ordinary differential equations: Runge–Kutta, collocation and multistep methods [1]. However, brief reflection demonstrates that the highly oscillatory nature of the forcing term necessitates the use of an exceedingly small step size. Thus, for simplicity let us assume that we are solving the delay differential problem

$$\boldsymbol{y}'(t) = \boldsymbol{f}(t, \boldsymbol{y}(t), \boldsymbol{y}(t-1))$$

with the Euler method

$$\boldsymbol{y}_{n+1} = \boldsymbol{y}_n + h\boldsymbol{f}(nh, \boldsymbol{y}_n, \boldsymbol{y}_{n-M}),$$

where we have used the constant step $h = 1/M,\ M \in \mathbb{N}$, and $\boldsymbol{y}_n \approx \boldsymbol{y}(nh)$. It is well known that the local truncation error scales like $h^2\boldsymbol{y}''(nh)$, hence the global error scales like $h\boldsymbol{y}''(nh)$. For the highly oscillatory system (1.1) we have $\boldsymbol{f}(t, \boldsymbol{y}(t), \boldsymbol{y}(t-1)) = A\boldsymbol{y}(t) + B\boldsymbol{y}(t-1) + \sum_{m=-\infty}^{\infty} \boldsymbol{a}_m(t)\mathrm{e}^{\mathrm{i}m\omega t}$ and it is easy to ascertain that

$$\boldsymbol{y}''(t) = \frac{\mathrm{d}}{\mathrm{d}t}\boldsymbol{f}(t, \boldsymbol{y}(t), \boldsymbol{y}(t-1)) \approx \mathrm{i}\omega \sum_{m=-\infty}^{\infty} m\boldsymbol{a}_m(t)\mathrm{e}^{\mathrm{i}m\omega t}, \qquad \omega \gg 1,$$

scales like ω. Therefore, to entertain any hope of reasonable precision we are compelled to choose a very small $h\omega$. A similar state of affairs prevails for all integration methods based upon B-series, inclusive of multistep and Runge–Kutta methods and Taylor expansions. Moreover, standard error-control and adaptation techniques, as used in modern advanced ODE and DDE software, are of little use because the error-control mechanism is bound to select a very small step size, consistent with $h\omega \ll 1$. Using such methods and software for (1.1)

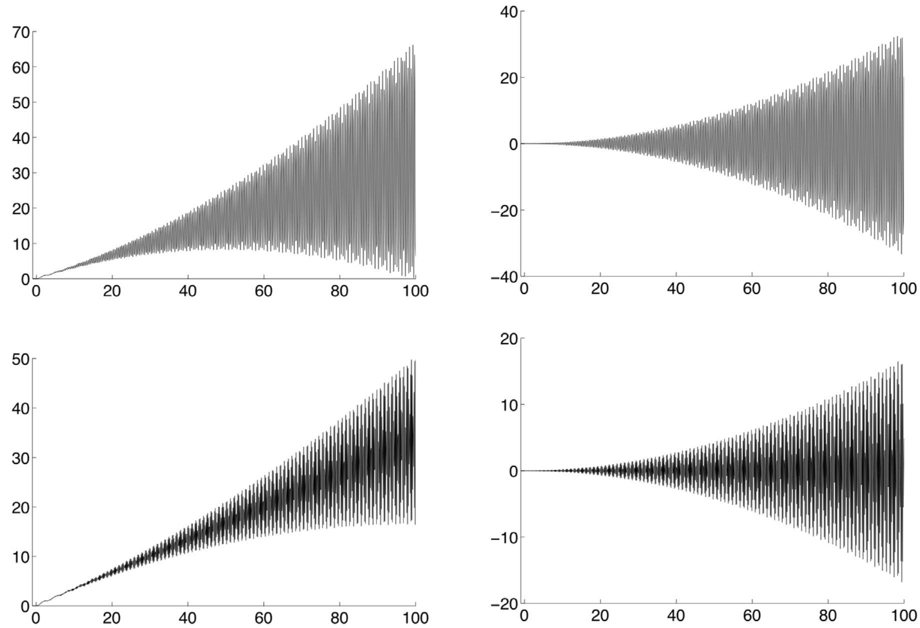

FIGURE 1. Real (on the left) and imaginary (on the right) parts of the solution of (1.3) for $\omega = 50$ (top row) and $\omega = 100$.

and similar highly oscillatory systems is not just exceedingly slow and expensive but also, once the interval of integration $[0, T]$ is sufficiently long, leads to substantial roundoff error accumulation and global error in excess of user-supplied tolerance. All this makes a compelling case for the development of a completely different breed of methods, dedicated to highly oscillatory systems and based upon completely different premises.

To illustrate our point and flesh out some numbers, let us consider the scalar equation

$$\left.\begin{aligned} &y'(t) = -y(t) - 2y(t-1) + t + (t+1)^2 \mathrm{e}^{6\mathrm{i}\omega t} - \mathrm{i}\mathrm{e}^{-10\mathrm{i}\omega t}; && t \in [0, T], \\ &y(t) = \varphi(t) && t \in [-1, 0]. \end{aligned}\right\} \tag{1.3}$$

The real and imaginary parts of the solution for $\omega = 50$ are displayed in Figure 1 and, unsurprisingly, they exhibit high oscillation.

We have approximated the solution of (1.3) for $\omega = 50$ (a fairly gentle oscillation) and $\varphi \equiv 0$ using the standard MATLAB routine `dde23`, which is an implementation of a Runge–Kutta method with variable step size and error control. The errors for absolute tolerances of $10^{-3}, 10^{-6}$ and 10^{-9} are displayed in Figure 2. It is evident that, regardless of user-specified tolerance, `dde23` delivers pointwise error of $\mathcal{O}(1)$: not even a single significant digit is recovered correctly. We should perhaps add that the entire pointless exercise took between 628 and 1057 s.

For comparison, we have solved (1.3) using the asymptotic-numerical method which we describe in Section 2 for different values of the parameter p. Not wishing to pre-empt subsequent discussion, we just observe that p denotes the number of 'asymptotic layers' in the representation of the solution of (1.1). The errors decrease rapidly with p (they grow in time at a similar rate to the growth of $|y(t)|$, *cf.* Fig. 1). Note that the run-times of the four methods were just 0.472, 0.810, 1.074 and 1.247 s, respectively.

A major feature of the methodology of this paper is that the higher the oscillation, the smaller the error. The accuracy for $\omega = 100$ is thus higher than in Figure 3. The run-times are virtually the same as for $\omega = 50$: 0.508, 0.779, 0.994 and 1.190 s respectively, while the pointwise accuracy improves. It goes without saying that

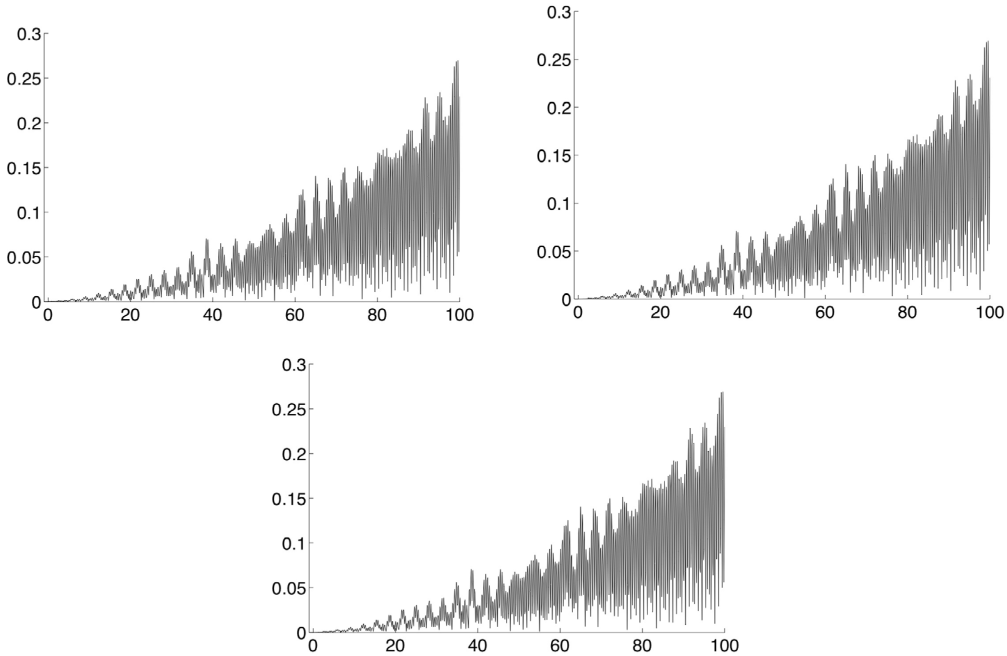

FIGURE 2. Absolute values of errors in the solution of (1.3) with $\omega = 50$, using `dde23` with `AbsTol` $= 10^{-3}, 10^{-6}, 10^{-9}$.

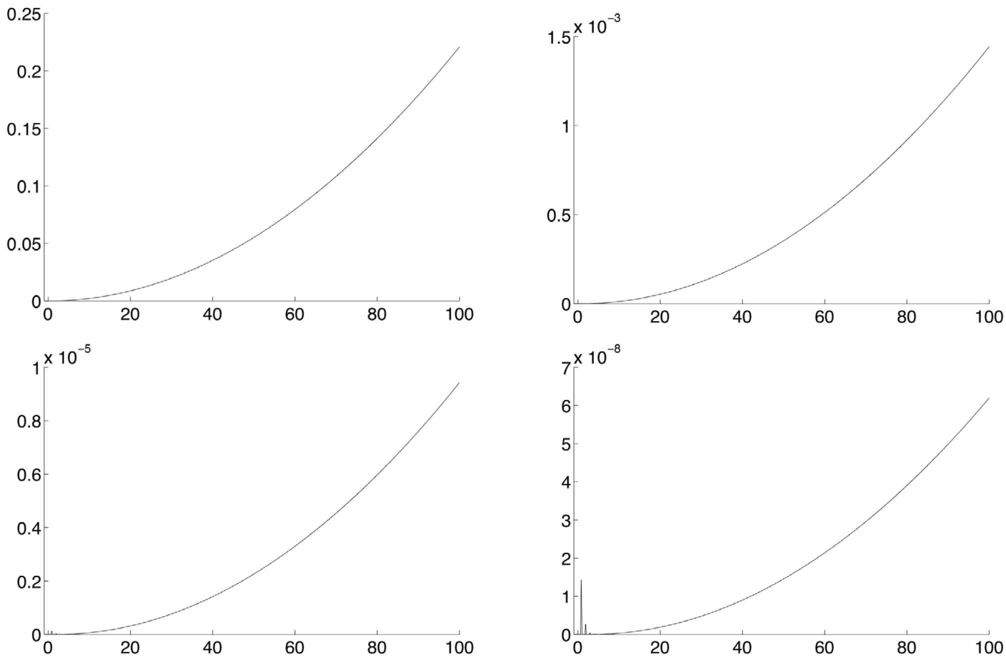

FIGURE 3. Absolute values of errors in the solution of (1.3) with $\omega = 50$, using our method with $p = 1, 2$ (top row) and $p = 3, 4$.

dde23 delivers an equally useless solution, regardless of user-provided tolerance, in this setting, except that the run-time for $\omega = 100$ is more than doubled.

Our ultimate goal is to develop asymptotic-numerical methodology for nonlinear equations of the form

$$\boldsymbol{y}'(t) = \boldsymbol{f}(t, \boldsymbol{y}(t), \boldsymbol{y}(t-1)) + \mathcal{A}_\omega(t)\boldsymbol{g}(t, \boldsymbol{y}(t), \boldsymbol{y}(t-1)), \tag{1.4}$$

where $\mathcal{A}_\omega$ is a $d \times d$ matrix with MFE entries, $(\mathcal{A}_\omega)_{k,\ell} = \sum_{m=-\infty}^{\infty} a_m^{k,\ell}(t)\mathrm{e}^{\mathrm{i}m\omega t}$, and with the initial condition (1.2). Inasmuch as the solution of linear equations like (1.1) is interesting on its merit, our main concern is in laying the foundations toward asymptotic and numerical solution of nonlinear equations like (1.4).

2. Asymptotic expansion and asymptotic-numerical methods

2.1. Asymptotic expansions for ODEs

Our starting point is the highly oscillatory ordinary differential system

$$\boldsymbol{y}' = \boldsymbol{f}(t, \boldsymbol{y}) + \sum_{m=-\infty}^{\infty} \boldsymbol{a}_m(t)\mathrm{e}^{\mathrm{i}m\omega t}, \quad 0 \le t \le T, \qquad \boldsymbol{y}(0) = \boldsymbol{y}_0, \tag{2.1}$$

whose solution can be expanded asymptotically,

$$\boldsymbol{y}(t) \sim \boldsymbol{p}_{0,0}(t) + \sum_{r=1}^{\infty} \frac{1}{\omega^r} \sum_{m=-\infty}^{\infty} \boldsymbol{p}_{r,m}(t)\mathrm{e}^{\mathrm{i}m\omega t} \tag{2.2}$$

[7]. The functions $\boldsymbol{p}_{r,m}$ are all independent of ω, hence non-oscillatory. For $m = 0$ they can be obtained by solving a non-oscillatory ordinary differential equation, while for $m \neq 0$ we find them by recursion. The important feature of (2.2) is thus that its building blocks, the functions $\boldsymbol{p}_{r,m}$, can be derived without any reference to ω and the latter enters the calculation only once the asymptotic expansion is computed for a specific value of t. Therefore, the expansion actually *improves* as ω becomes large. This might be surprising to those used to methods based upon Taylor expansions but should come as little surprise to practitioners of asymptotic analysis.

Another important feature of (2.2), which is shared by asymptotic expansions of DDEs, is that the solution consists of amplitude-$\mathcal{O}(\omega^{-1})$ oscillations superimposed upon the non-oscillatory function $\boldsymbol{p}_{0,0}$.

2.2. Asymptotic expansion of (1.1)

We wish to emulate the asymptotic expansion (2.2) in the setting of delay differential equations. Unfortunately, this model is much too simple for our needs. Our basic *ansatz,* valid for both the ODE (2.1) and the DDE (1.2) is that

$$\boldsymbol{y}(t) \sim \boldsymbol{p}(t) + \sum_{r=1}^{\infty} \frac{1}{\omega^r} \boldsymbol{\psi}_r(t, \omega), \qquad \omega \gg 1. \tag{2.3}$$

Note that the $\boldsymbol{\psi}_r(t)$s depend on ω, but we stipulate that $\boldsymbol{\psi}_r(t) = \mathcal{O}(1)$, $\omega \gg 1$, for all $r \in \mathbb{Z}_+$. Knowing the structure of the forcing term, it seems reasonable to look for functions $\boldsymbol{\psi}_r$ which are somehow related to modulated Fourier expansions. Before presenting the precise form of functions $\boldsymbol{\psi}_r$ which occur in the DDE case, we need to define the following sets,

$$\mathbb{M} = \{0\} \cup \{m \in \mathbb{Z} \,:\, \boldsymbol{a}_m \not\equiv \boldsymbol{0} \text{ on } [0, T]\},$$

$$\mathbb{I}_r = \begin{cases} \{(0, m) \,:\, m \in \mathbb{M}\}, & r = 1, \\ \{(jm, m) \,:\, j \in \{0, 1, \ldots, r-1\},\ m \in \mathbb{M} \setminus \{0\}\} \cup \{(m, 0) \,:\, m \in \mathbb{M}\}, & r \geq 2. \end{cases}$$

The set $\mathbb{M}$ consists of 'active' coefficients $\boldsymbol{a}_m$, while $\mathbb{I}_r$ has no deep significance beyond making our notation simpler. The functions $\boldsymbol{\psi}_r$ for $r \geq 1$ are of the form

$$\boldsymbol{\psi}_r(t,\omega) = \sum_{(l,m)\in\mathbb{I}_r} \boldsymbol{b}_m^{r,l}(t) e^{\mathrm{i}\omega(mt-l)}, \qquad r \geq 1. \tag{2.4}$$

The major task ahead of us is to identify $\boldsymbol{p}(t)$, $t > 0$, and $\boldsymbol{b}_m^{r,l}$ for $t \geq 0$, $r \geq 1$, $(l,m) \in \mathbb{I}_r$.

2.3. Explicit form of the asymptotic expansion

In this subsection we are deriving explicit formulæ for the functions $\boldsymbol{p}(t)$ and $\boldsymbol{b}_m^{r,l}(t)$, $r = 0, 1, \ldots, \infty$. For the convenience of reader and eventual application to the numerical solution of the DDE (1.1), it is convenient to obtain those coefficients in an algorithmic manner. The first two coefficients are in an explicit form

$$\begin{aligned} \boldsymbol{p}'(t) &= A\boldsymbol{p}(t) + B\boldsymbol{p}(t-1) + \boldsymbol{a}_0(t), \qquad t \geq 0, \\ \boldsymbol{p}(t) &= \boldsymbol{\varphi}(t), \qquad t \in [-1, 0); \end{aligned} \tag{2.5}$$

$$\boldsymbol{b}_m^{1,0}(t) = \frac{\boldsymbol{a}_m(t)}{\mathrm{i}m}, \qquad m \neq 0, \tag{2.6}$$

and the general expressions for the functions $\boldsymbol{b}_m^{r,l}$ are

$$\begin{aligned} \boldsymbol{b}_0^{r,0\prime}(t) &= A\boldsymbol{b}_0^{r,0}(t) + B\boldsymbol{b}_0^{r,0}(t-1), \qquad t \geq 0, \\ \boldsymbol{b}_0^{r,0}(t) &\equiv 0, \qquad t \in [-1, 0), \\ \boldsymbol{b}_0^{r,0}(0) &= -\sum_{s\neq 0} \boldsymbol{b}_s^{r,0}(0); \end{aligned} \tag{2.7}$$

$$\begin{aligned} \boldsymbol{b}_0^{r,m\prime}(t) &= A\boldsymbol{b}_0^{r,m}(t) + B\boldsymbol{b}_0^{r,m}(t-1), \qquad t \geq 0, \quad m \neq 0, \\ \boldsymbol{b}_0^{r,m}(t) &\equiv 0, \qquad t \in [-1, 0), \\ \boldsymbol{b}_0^{r,m}(0) &= -\sum_{j=1}^{r-1} \boldsymbol{b}_m^{r,jm}(0), \end{aligned} \tag{2.8}$$

$$\boldsymbol{b}_m^{r,0}(t) = \frac{1}{\mathrm{i}m}[A\boldsymbol{b}_m^{r-1,0}(t) - \boldsymbol{b}_m^{r-1,0\prime}(t)], \qquad m \neq 0; \tag{2.9}$$

$$\begin{aligned} \boldsymbol{b}_m^{r,jm}(t) &= \frac{1}{\mathrm{i}m}[A\boldsymbol{b}_m^{r-1,jm}(t) + B\boldsymbol{b}_m^{r-1,(j-1)m}(t-1) - \boldsymbol{b}_m^{r-1,jm\prime}(t)], \\ & m \neq 0, \quad j = 1, 2, \ldots, r-2, \end{aligned} \tag{2.10}$$

$$\boldsymbol{b}_m^{r,(r-1)m}(t) = \frac{1}{\mathrm{i}m} B\boldsymbol{b}_m^{r-1,(r-2)m}(t-1), \qquad m \neq 0 \tag{2.11}$$

for all $r \geq 1$, except for $r = 1, l = 0$, $m \neq 0$, which has been already given by (2.6).

Note that ω is completely absent from our formulæ! Thus, both the differential equations for $\boldsymbol{p}$ and $\boldsymbol{b}_0^{r,l}$ and all the recursions for $\boldsymbol{b}_m^{r,l}$, $m \neq 0$, are non-oscillatory. The beauty and power of expressions (2.5)–(2.11) lies in their simplicity. Note that a single complicated, highly oscillatory delayed differential equation is replaced with recursive equations or delay differential equations which, being non-oscillatory, can be easily solved numerically with standard methods. Of course, practical application of (2.3) to numerical computation requires the truncation of the infinite sum, but this can be done in a transparent manner and, as we see in Section 3, restricting r to a very small range already yields an excellent approximation – one whose excellence *improves* once ω becomes larger.

We now proceed to derive (2.5)–(2.11) in a systematic manner. For simplicity of notation we henceforth omit the dependence on t of the functions in question and adopt the convention that placing a tilde on the top of a function means that it is evaluated at point $t-1$. Hence, $\boldsymbol{p}$ should be understood as $\boldsymbol{p}(t)$, while $\tilde{\boldsymbol{p}}$ stands for $\boldsymbol{p}(t-1)$.

Applying *ansatz* (2.2) to equation (1.1) we obtain

$$\boldsymbol{p}' + \sum_{(l,m)\in\mathbb{I}_1} \mathrm{i}m\boldsymbol{b}_m^{1,l}\mathrm{e}^{\mathrm{i}\omega(mt-l)} + \sum_{r=1}^{\infty}\frac{1}{\omega^r}\left[\sum_{(l,m)\in\mathbb{I}_r}\boldsymbol{b}_m^{r,l\prime}\mathrm{e}^{\mathrm{i}\omega(mt-l)} + \sum_{(l,m)\in\mathbb{I}_{r+1}}\mathrm{i}m\boldsymbol{b}_m^{r+1,l}\mathrm{e}^{\mathrm{i}\omega(mt-l)}\right]$$
$$= A\left[\boldsymbol{p} + \sum_{r=1}^{\infty}\frac{1}{\omega^r}\sum_{(l,m)\in\mathbb{I}_r}\boldsymbol{b}_m^{r,l}\mathrm{e}^{\mathrm{i}\omega(mt-l)}\right] + B\left[\tilde{\boldsymbol{p}} + \sum_{r=1}^{\infty}\frac{1}{\omega^r}\sum_{(l,m)\in\mathbb{I}_r}\tilde{\boldsymbol{b}}_m^{r,l}\mathrm{e}^{\mathrm{i}\omega(mt-l-m)}\right] + \sum_{m\in\mathbb{M}}\boldsymbol{a}_m\mathrm{e}^{\mathrm{i}\omega mt}. \quad (2.12)$$

We identify above two different kinds of scales: *magnitude,* expressed in power of ω, and *frequency,* namely terms of the form $\mathrm{e}^{\mathrm{i}\omega mt}$ for distinct m. The first stage is to separate magnitudes and, next, separate frequencies. We let

$$\tilde{\mathbb{I}}_r = \{(l,m)\in\mathbb{I}_r \;:\; m\neq 0\}\subset\mathbb{I}_r, \qquad r\in\mathbb{N}.$$

2.3.1. The zeroth term

We commence by collecting the $\mathcal{O}(1)$ (in ω) terms in (2.12). The outcome is

$$\boldsymbol{p}' + \sum_{(l,m)\in\tilde{\mathbb{I}}_1}\mathrm{i}m\boldsymbol{b}_m^{1,l}\mathrm{e}^{\mathrm{i}\omega(mt-l)} = A\boldsymbol{p}(t) + B\boldsymbol{p}(t-1) + \boldsymbol{a}_0(t) + \sum_{m\in\mathbb{M}\setminus\{0\}}\boldsymbol{a}_m(t)\mathrm{e}^{\mathrm{i}\omega mt}.$$

Next we separate frequencies. $m=0$ yields (2.5), while $m\in\tilde{I}_1$ results in (2.6).

2.3.2. The $r=1$ term

Now we pull out of (2.12) the coefficients of magnitude $\mathcal{O}(\omega^{-1})$. The outcome is

$$\sum_{(l,m)\in\mathbb{I}_1}\boldsymbol{b}_{\boldsymbol{m}}^{\boldsymbol{1},\boldsymbol{l}\prime}\mathrm{e}^{\mathrm{i}\omega(mt-l)} + \sum_{(l,m)\in\mathbb{I}_2}\mathrm{i}m\boldsymbol{b}_m^{2,l}\mathrm{e}^{\mathrm{i}\omega(mt-l)} = A\sum_{(l,m)\in\mathbb{I}_1}\boldsymbol{b}_m^{1,l}\mathrm{e}^{\mathrm{i}\omega(mt-l)} + B\sum_{(l,m)\in\mathbb{I}_1}\tilde{\boldsymbol{b}}_m^{1,l}\mathrm{e}^{\mathrm{i}\omega(mt-l-m)}.$$

Since $\mathbb{I}_1 = \{(0,m);\; m\in\mathbb{M}\}$ and $\mathbb{I}_2 = \{(0,m),(m,m),(m,0);\; m\in\mathbb{M}\}$, this is equivalent to

$$\sum_{(0,m)\in\tilde{\mathbb{I}}_1}\boldsymbol{b}_m^{1,0\prime}\mathrm{e}^{\mathrm{i}\omega mt} + \sum_{(0,0)\in\mathbb{I}_1}\boldsymbol{b}_0^{1,0\prime} + \sum_{(m,m)\in\mathbb{I}_2\setminus\mathbb{I}_1}\mathrm{i}m\boldsymbol{b}_m^{2,m}\mathrm{e}^{\mathrm{i}\omega m(t-1)} + \sum_{(0,m)\in\tilde{\mathbb{I}}_1}\mathrm{i}m\boldsymbol{b}_m^{2,0}\mathrm{e}^{\mathrm{i}\omega mt}$$
$$= A\sum_{(0,m)\in\tilde{\mathbb{I}}_1}\boldsymbol{b}_m^{1,0}\mathrm{e}^{\mathrm{i}\omega mt} + A\sum_{(0,0)\in\mathbb{I}_1}\boldsymbol{b}_0^{1,0} + B\sum_{(0,m)\in\tilde{\mathbb{I}}_1}\tilde{\boldsymbol{b}}_m^{1,0}\mathrm{e}^{\mathrm{i}\omega m(t-1)} + B\sum_{(0,0)\in\mathbb{I}_1}\tilde{\boldsymbol{b}}_0^{1,0}.$$

Bearing in mind the definitions of $\mathbb{I}_1$, $\mathbb{I}_2$ and $\tilde{\mathbb{I}}_1$, we thus have

$$\begin{aligned}
\boldsymbol{b}_0^{1,0\prime} &= A\boldsymbol{b}_0^{1,0} + B\tilde{\boldsymbol{b}}_0^{1,0},\\
\boldsymbol{b}_m^{2,0} &= \frac{1}{\mathrm{i}m}[A\boldsymbol{b}_m^{1,0} - \boldsymbol{b}_m^{1,0\prime}], \qquad m\neq 0,\\
\boldsymbol{b}_m^{2,m} &= \frac{1}{\mathrm{i}m}B\tilde{\boldsymbol{b}}_m^{1,0}, \qquad m\neq 0,
\end{aligned}$$

consistently with (2.7), (2.9) and (2.11), respectively. Finally, the initial conditions for $\boldsymbol{b}_0^{1,0}$ follow from the condition

$$\boldsymbol{\psi}_r(t,\omega)\equiv 0, \qquad t\in[-1,0], \qquad r\geq 1, \quad (2.13)$$

which is implied by $\boldsymbol{p}(t)=\boldsymbol{\varphi}(t)$, $t\in[-1,0]$, and $\boldsymbol{\psi}_r=\mathcal{O}(1)$, $\omega\gg 1$.

2.3.3. The $r=2$ term

We note the pattern: for any r we obtain a DDE for $\boldsymbol{b}_0^{r,l}$ and recurrence relations for $\boldsymbol{b}_m^{r+1,l}$, $m\neq 0$. This is also the case for $r=2$. Collecting $\mathcal{O}\big(\omega^{-2}\big)$ terms, we thus have

$$\begin{aligned}
&\sum_{(0,m)\in\tilde{\mathbb{I}}_2}\boldsymbol{b}_m^{2,0\prime}\mathrm{e}^{\mathrm{i}\omega mt}+\sum_{(m,m)\in\tilde{\mathbb{I}}_2}\boldsymbol{b}_m^{2,m\prime}\mathrm{e}^{\mathrm{i}\omega m(t-1)}+\sum_{(l,0)\in\mathbb{I}_2\setminus\tilde{\mathbb{I}}_2}\boldsymbol{b}_0^{2,l\prime}\mathrm{e}^{-\mathrm{i}\omega l}\\
&+\sum_{(0,m)\in\tilde{\mathbb{I}}_2}\mathrm{i}m\boldsymbol{b}_m^{3,0}\mathrm{e}^{\mathrm{i}m\omega t}+\sum_{(m,m)\in\tilde{\mathbb{I}}_2}\mathrm{i}m\boldsymbol{b}_m^{3,m}\mathrm{e}^{\mathrm{i}\omega m(t-1)}+\sum_{(2m,m)\in\tilde{\mathbb{I}}_3}\mathrm{i}m\boldsymbol{b}_m^{3,2m}\mathrm{e}^{\mathrm{i}\omega m(t-2)}\\
=\;&A\sum_{(0,m)\in\tilde{\mathbb{I}}_2}\boldsymbol{b}_m^{2,0}\mathrm{e}^{\mathrm{i}\omega mt}+A\sum_{(l,0)\in\mathbb{I}_2}\boldsymbol{b}_0^{2,l}\mathrm{e}^{-\mathrm{i}\omega l}+A\sum_{(m,m)\in\mathbb{I}_2}\boldsymbol{b}_m^{2,m}\mathrm{e}^{\mathrm{i}\omega m(t-1)}\\
&+B\sum_{(0,m)\in\tilde{\mathbb{I}}_2}\tilde{\boldsymbol{b}}_m^{2,0}\mathrm{e}^{\mathrm{i}\omega m(t-1)}+B\sum_{(l,0)\in\mathbb{I}_2}\tilde{\boldsymbol{b}}_0^{2,l}\mathrm{e}^{-\mathrm{i}\omega l}+B\sum_{(m,m)\in\mathbb{I}_2}\tilde{\boldsymbol{b}}_m^{2,m}\mathrm{e}^{\mathrm{i}\omega m(t-2)},
\end{aligned}$$

where $\mathbb{I}_3=\{(0,m),(m,m),(2m,m),(m,0)\,:\,m\in\mathbb{M}\}$.

Separating frequencies, we have the following:

$$\begin{aligned}
\mathrm{e}^{-\mathrm{i}\omega m}:&\;\boldsymbol{b}_0^{2,m\prime}=A\boldsymbol{b}_0^{2,m}+B\tilde{\boldsymbol{b}}_0^{2,m}, && m\in\mathbb{Z},\\
\mathrm{e}^{\mathrm{i}m\omega t}:&\;\boldsymbol{b}_m^{3,0}=\frac{1}{\mathrm{i}m}(A\boldsymbol{b}_m^{2,0}-\boldsymbol{b}_m^{2,0\prime}), && m\neq 0,\\
\mathrm{e}^{\mathrm{i}\omega m(t-1)}:&\;\boldsymbol{b}_m^{3,m}=\frac{1}{\mathrm{i}m}(A\boldsymbol{b}_m^{2,m}+B\tilde{\boldsymbol{b}}_m^{2,m}-\boldsymbol{b}_m^{2,m\prime}), && m\neq 0,\\
\mathrm{e}^{\mathrm{i}\omega m(t-2)}:&\;\boldsymbol{b}_m^{3,2m}=\frac{1}{\mathrm{i}m}B\tilde{\boldsymbol{b}}_m^{2,m}, && m\neq 0.
\end{aligned}$$

The initial conditions for the DDEs follow from (2.13) and all is consistent with (2.7)–(2.11).

2.3.4. The r-th term

We have already done the heavy lifting: the general case follows identically to $r=2$. Thus,

$$\mathbb{I}_{r-1}=\{(0,m),(m,m),\ldots,((r-2)m,m),(m,0)\,:\,m\in\mathbb{M}\}$$

and

$$\begin{aligned}
&\sum_{j=0}^{r-1}\sum_{m\neq 0}\boldsymbol{b}_m^{r,jm\prime}\mathrm{e}^{\mathrm{i}\omega m(t-j)}+\sum_{m=-\infty}^{\infty}\boldsymbol{b}_0^{r,m\prime}\mathrm{e}^{-\mathrm{i}\omega m}+\sum_{j=0}^{r}\sum_{m\neq 0}\mathbf{i}m\boldsymbol{b}_m^{r+1,jm}\mathrm{e}^{\mathrm{i}m\omega(t-j)}\\
=\;&A\sum_{j=0}^{r-1}\sum_{m=-\infty}^{\infty}\boldsymbol{b}_m^{r,jm}\mathrm{e}^{\mathrm{i}\omega m(t-j)}+A\sum_{m=-\infty}^{\infty}\boldsymbol{b}_0^{r,m}\mathrm{e}^{-\mathrm{i}\omega m}\\
&+B\sum_{j=1}^{r}\sum_{m=-\infty}^{\infty}\tilde{\boldsymbol{b}}_m^{r,(j-1)m}\mathrm{e}^{\mathrm{i}m\omega(t-j)}+B\sum_{m=-\infty}^{\infty}\tilde{\boldsymbol{b}}_0^{r,m}\mathrm{e}^{-\mathrm{i}\omega m}.
\end{aligned}$$

Again we separate the frequencies and the outcome is

$$\begin{aligned}
\mathrm{e}^{-\mathrm{i}\omega m}:&\quad\boldsymbol{b}_0^{r,m\prime}=A\boldsymbol{b}_0^{r,m}+B\tilde{\boldsymbol{b}}_0^{r,m}, && m\in\mathbb{Z},\\
\mathrm{e}^{\mathrm{i}\omega mt}:&\quad\boldsymbol{b}_m^{r+1,0}=\frac{1}{\mathrm{i}m}(A\boldsymbol{b}_m^{r,0}-\boldsymbol{b}_m^{r,0\prime}), && m\neq 0,\\
\mathrm{e}^{\mathrm{i}\omega m(t-j)}:&\quad\boldsymbol{b}_m^{r+1,jm}=\frac{1}{\mathrm{i}m}(A\boldsymbol{b}_m^{r,jm}+B\tilde{\boldsymbol{b}}_m^{r,(j-1)m}-\boldsymbol{b}_m^{r,jm\prime}), && j=1,\ldots,r-1,\ m\neq 0,\\
\mathrm{e}^{\mathrm{i}\omega m(t-r)}:&\quad\boldsymbol{b}_m^{r+1,rm}=\frac{1}{\mathrm{i}m}B\tilde{\boldsymbol{b}}_m^{r,(r-1)m}, && m\neq 0.
\end{aligned}$$

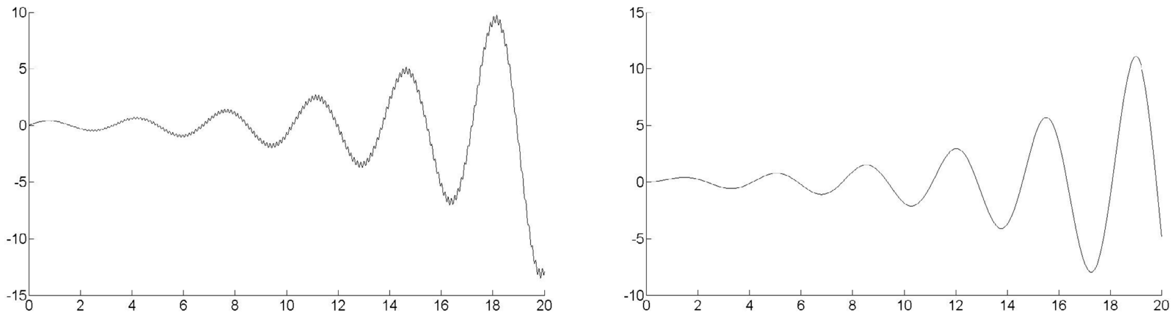

FIGURE 4. The real and imaginary parts of the solution of (3.1) for $\omega = 50$.

This, together with initial conditions derived from (2.13), is precisely (2.7)–(2.11) with appropriately shifted index r, confirming the validity of the DDEs and recurrence relations which, in their totality, result in the asymptotic expansion (2.3)–(2.4).

2.4. An asymptotic-numerical method

The numerical implementation of the asymptotic expansion (2.3–4) requires three different truncations. Firstly, we need to replace the right-hand side of (2.3) by a finite sum,

$$\boldsymbol{y}(t) \approx \boldsymbol{p}(t) + \sum_{r=1}^{p} \frac{1}{\omega^r} \boldsymbol{\psi}_r(t,\omega). \tag{2.14}$$

Note that fairly small values of $p \geq 1$ are perfectly adequate: in Section 1 we have used $p = 1$ even with fairly small ω, yet the results were very good indeed. Secondly, we need to restrict the set $\mathbb{M}$, hence also $\mathbb{I}_r$, $r = 1, \ldots, p$ to

$$\mathbb{M}_s = \{m \in \mathbb{M} \,:\, |m| \leq s\}$$

for suitably large $s \geq 1$. Note that many sets $\mathbb{M}$ in applications are already finite and there is no need to truncate them. Finally, we need to solve (2.5) and (2.7)–(2.8) numerically: given that these are non-oscillatory linear DDEs, this can be done with great ease using existing methods and software.

Note that, at least in principle, we can use just one expansion (2.14) in the entire interval of interest $[0, T]$. This is not a good idea: (2.3) is an asymptotic expansion, hence we cannot be assured of convergence in exceedingly long intervals. Although precise analysis, even in an ODE case, is not yet available, computational experience indicates that a good policy is to cover $[0, T]$ with a fairly small number of large time steps. In each time step we re-compute the functions $\boldsymbol{p}$ and $\boldsymbol{b}_m^{r,l}$ in the requisite range – of course, we no longer start at the origin, but this represents no problem whatsoever.

3. A FEW EXAMPLES

It is a sound policy to try any new computational tool on a number of examples: although general theory assures us of the efficacy of our approach, numerical experimentation might well highlight potential problems. Moreover, in the case of DDEs (1.1), there is very little experience which sort of solution to expect, hence the merit in using the approach of Section 2 as an exploratory tool.

All computations in this section have been performed using (2.14) with $p = 6$. The DDEs, required to derive expansion terms in (2.14), have been computed with `dde23` using very small bound on absolute error. Given

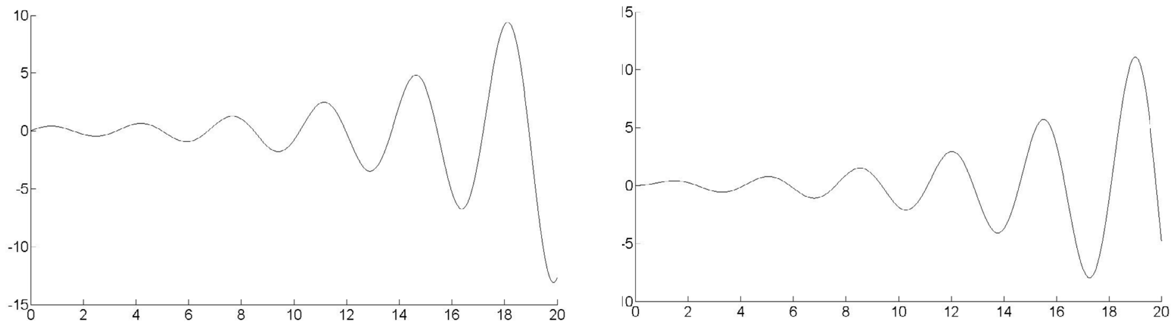

FIGURE 5. The real and imaginary parts of the solution of (3.1) for $\omega = 10^4$.

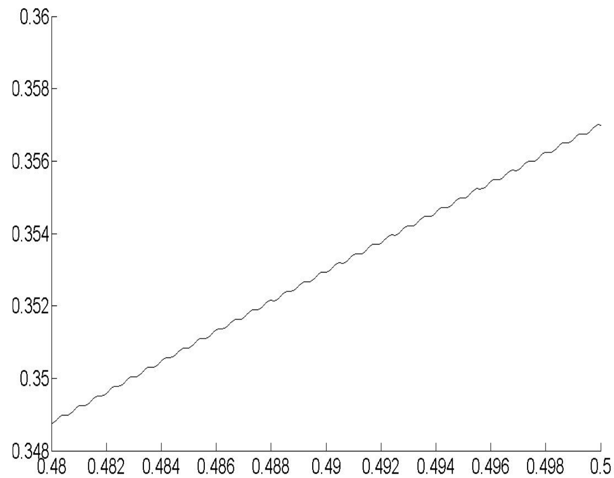

FIGURE 6. The real part of the solution of (3.1) for $\omega = 10^4$ in a very small sub-interval: note that the oscillations are now visible.

that these DDEs are all non-oscillatory, this has resulted in very small – practically, negligible – global error and the computation itself is extraordinarily rapid.

We commence from the scalar equation

$$\begin{aligned} y'(t) &= \mathrm{i}y(t) - y(t-1) + t\sin\omega t, \qquad 0 < t \le 20, \\ y(t) &= \mathrm{e}^{\mathrm{i}t}, \qquad -1 \le t \le 0. \end{aligned} \tag{3.1}$$

The forcing term can be easily represented as a modulated Fourier series, $a_{-1}(t) = \frac{1}{2}\mathrm{i}t$, $a_1(t) = -\frac{1}{2}\mathrm{i}t$, $a_m \equiv 0$ for $|m| \neq 1$. Note that the amplitude of the forcing term grows linearly and we expect to see this expressed in the exact solution.

We commence from a fairly modest oscillation, $\omega = 50$. The real and imaginary parts of the solution are displayed in Figure 4. It is evident that the amplitude lives within a linearly-increasing envelope, in line with the linear increase in the amplitude of the forcing term. Moreover, it can be easily seen that the solution consists of a smooth component overlaid by small-amplitude rapid oscillations: all this is in line with the theory of the last section. (The oscillations are easily visible only in the real part, but this is purely a matter of plotting resolution: read on).

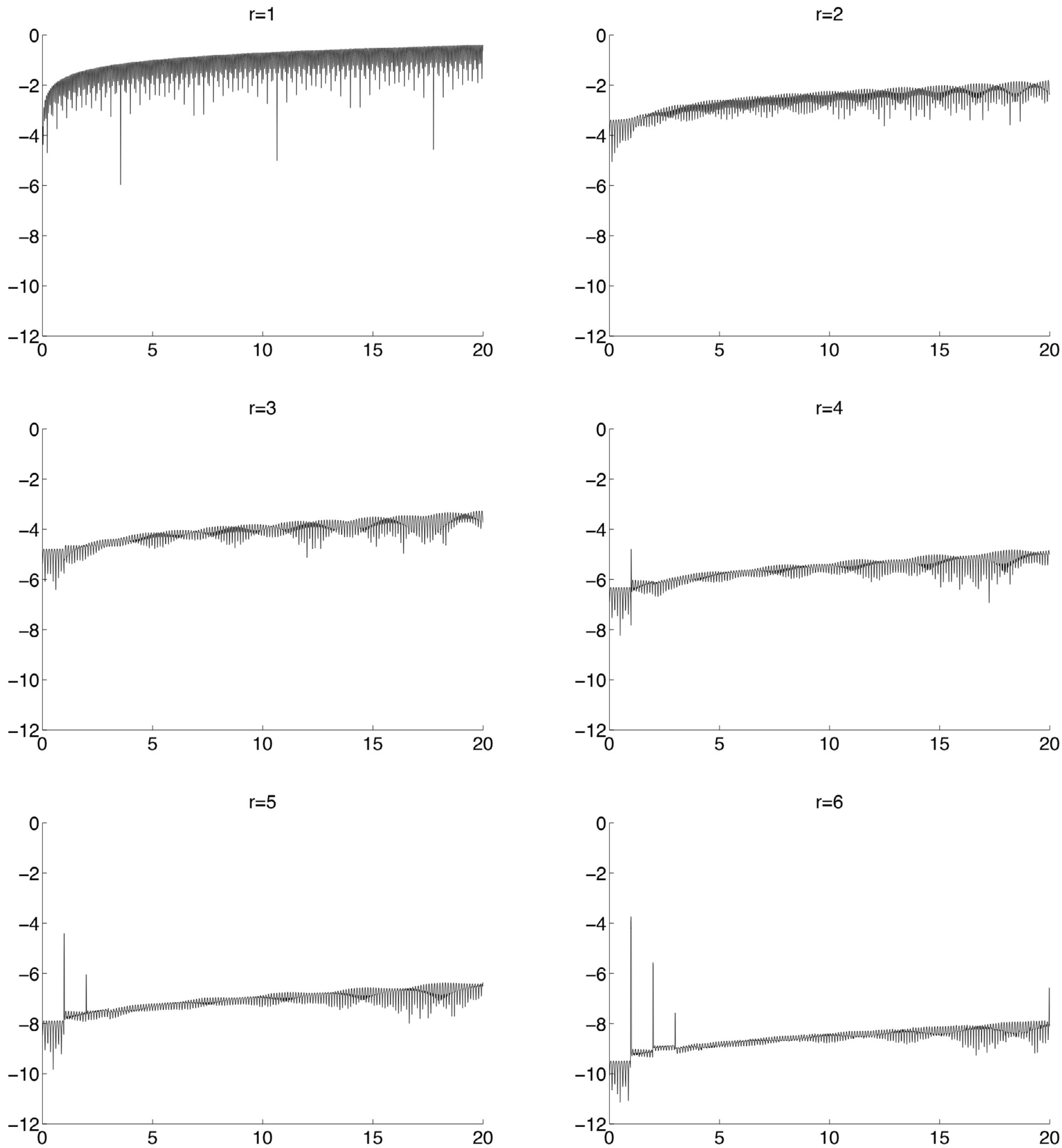

FIGURE 7. The size $\log_{10}|\psi_r(t,\omega)|$ of the consecutive 'layers' in (2.14) for equation (3.1) with $\omega = 10^4$.

Next we increase ω in (3.1) two hundred-fold, to $\omega = 10\,000$. We are now within a regime that is bound to defeat standard numerical methods: bearing in mind the discussion in Section 1, a reasonable choice of step-size $h > 0$ in a classical numerical method must satisfy $h\omega \ll 1$. Indeed, wishing to obtain an error less than a user-supplied tolerance $\mathtt{TOL}$, a good rule of a thumb is to choose $h = \rho \cdot \mathtt{TOL}^{1/p}\omega^{-1}$, where p is the (classical) order of the classical method and $\rho \in (0,1)$. In the case of the Euler method of Section 1, $\mathtt{TOL} = 10^{-6}$ means

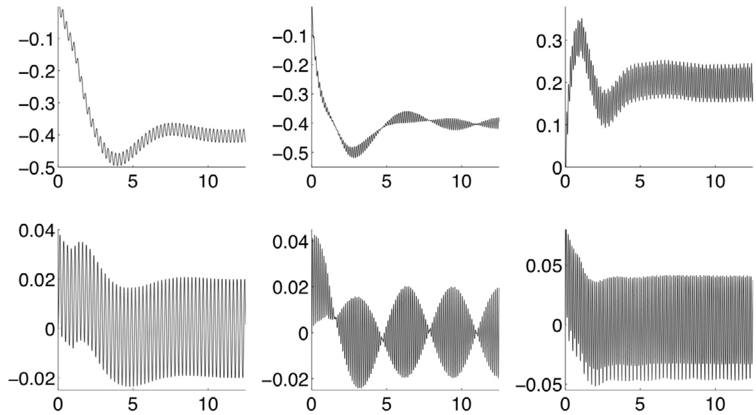

FIGURE 8. Real (top row) and imaginary parts of the three components of the solution of the system (3.2) with $\omega = 25$, using $p = 6$.

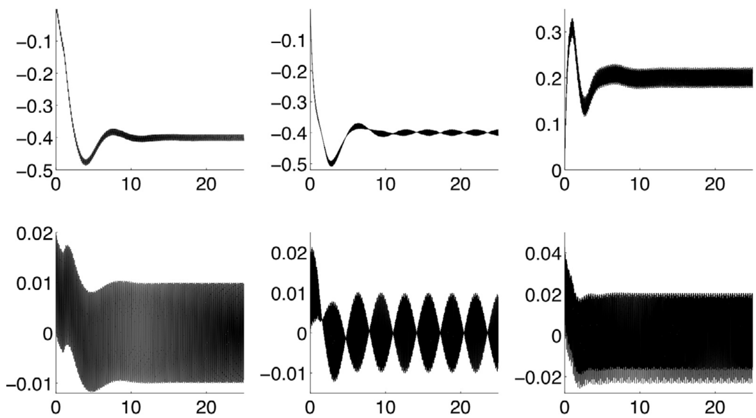

FIGURE 9. Real (top row) and imaginary parts of the three components of the solution of the system (3.2) with $\omega = 50$, using $p = 6$.

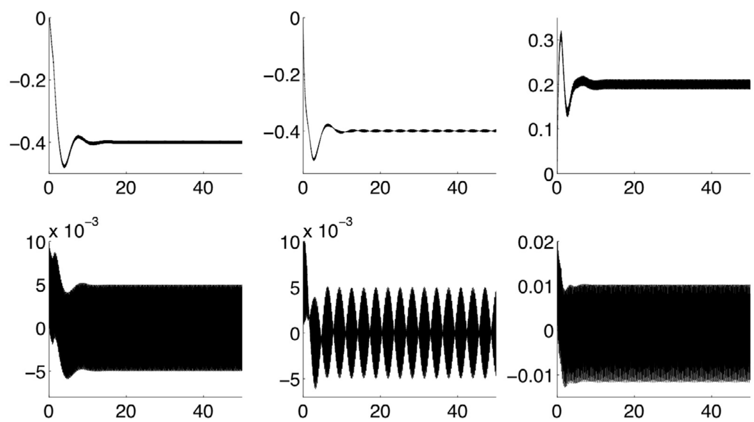

FIGURE 10. Real (top row) and imaginary parts of the three components of the solution of the system (3.2) with $\omega = 100$, using $p = 6$.

$h < 10^{-10}$. This leads to prohibitive cost. Worse, given the sheer number of floating-point operations, such a small step-size results in very significant round-off error, which is bound to render any estimate of global error fairly meaningless.

Unlike classical methods, the asymptotic-numerical solver (2.14) remains robust – actually, improves – for large ω, while the run-time (for fixed p) is independent of ω. Real and imaginary parts of the solution are displayed in Figure 5.

Comparing Figures 4 and 5, we note that the solution is almost identical, the only difference being that the small-amplitude oscillations in Figure 4 seem to have disappeared altogether in Figure 5. This, of course, is an illusion: the oscillations have not gone away, their amplitude just became *very* small indeed, roughly $\approx 10^{-4}$. Thus, they are simply too small to be seen in Figure 5. However, once we focus on a much smaller time interval, the oscillations are visible with the naked eye. Thus, in Figure 6 we have displayed the solution of (3.1) with $\omega = 10^4$ in a very small time interval. Because the function $p(t)$ varies there very moderately, small-amplitude oscillations overlaying it can be easily seen. Of course, the fact that we cannot see the oscillations does not mean that somehow they are 'invisible' to a classical numerical method.

In Figure 7 we have displayed the size of the 'layers' in formula (2.14), *i.e.* plotted $\log_{10}|\psi_r(t,\omega)|$ for equation (3.1), $\omega = 10^4$ and $r = 1, \ldots, 6$. To illustrate the rate of decay in the amplitude for increasing r, we have plotted all graphs with the same vertical axis. The oscillation is evident – as is evident that the amplitude decreases with r, in line with the reasoning underlying our methodology. We also observe that for large rs there are unwelcome jumps in amplitude at integer points and that the magnitude of these jumps decays rapidly as the time increases. Although no comprehensive explanation of this behaviour is available, it makes sense that it is connected to the regularity of the solutions of DDEs: it is well known that that kth derivative of $\boldsymbol{y}$ in (1.1) may be discontinuous at $t = k$, $k \in \mathbb{Z}_+$. The likely culprit is not the formula (2.14) *per se* but a deterioration in the accuracy of the numerical method used to solve the non-oscillatory systems (2.5), (2.7) and (2.8) at integer points.

Our last example is the highly oscillatory DDE system (1.1), where

$$A = \begin{bmatrix} -2 & 1 & 0 \\ 1 & -2 & 1 \\ 0 & 1 & -2 \end{bmatrix}, \qquad B = \begin{bmatrix} 0 & 1 & 0 \\ -1 & 0 & 0 \\ 0 & 0 & -1 \end{bmatrix}, \tag{3.2}$$
$$\boldsymbol{a}_{-2} = \begin{bmatrix} 0 \\ 0 \\ -2 \end{bmatrix}, \quad \boldsymbol{a}_0 = \begin{bmatrix} 0 \\ -1 \\ 1 \end{bmatrix}, \quad \boldsymbol{a}_1 = \begin{bmatrix} \frac{1}{2} \\ 0 \\ 0 \end{bmatrix}, \quad \boldsymbol{a}_2 = \begin{bmatrix} 0 \\ \cos t \\ 0 \end{bmatrix}, \quad \boldsymbol{a}_3 = \begin{bmatrix} 0 \\ 0 \\ \frac{1}{2} \end{bmatrix},$$

otherwise $\boldsymbol{a}_m = \mathbf{0}$, with zero initial condition in $(-1, 0]$.

Figures 8–10 exhibit the solution of the highly oscillatory DDE system (3.2) for three different values of ω. In each case we have used $p = 6$, solving non-oscillatory equations with `dde23` to very high accuracy. The oscillation in Figure 8 is fairly mild and, as we should already come to expect, it is of a fairly large amplitude. The amplitude is roughly halved in Figure 9, once the frequency ω is doubled (this behaviour is much more visible for the imaginary part, in the bottom row, which oscillates about the zero solution). It is halved again in Figure 10, consistently with our theory.

4. Conclusions

This paper represents a preliminary exploration of the very rich and unexplored area of delay-differential equations with highly oscillatory forcing. We have demonstrated that the solution of the linear system $\boldsymbol{y}'(t) = A\boldsymbol{y}(t) + B\boldsymbol{y}(t-1) + \sum_{m=-\infty}^{\infty} \boldsymbol{a}_m(t)\mathrm{e}^{\mathrm{i}m\omega t}$ can be expanded into asymptotic series in inverse powers of the frequency ω and that this expansion can be used as a cornerstone of a very effective numerical method.

The next stage in the exploration of DDEs with highly oscillatory forcing terms ventures into the realm of nonlinear equations of the form

$$\boldsymbol{y}'(t) = \boldsymbol{f}(t, \boldsymbol{y}(t), \boldsymbol{y}(t-1)) + \sum_{m=-\infty}^{\infty} \boldsymbol{a}_m(t)\mathrm{e}^{\mathrm{i}m\omega t}.$$

We expect to explore this issue in a future paper. Another outstanding challenge is to incorporate our theory, whether for linear or nonlinear DDEs, into practical applications in computational electronic engineering.

References

[1] A. Bellen and M. Zennaro, *Numerical Methods for Delay Differential Equations*. Oxford University Press, Oxford, UK (2003).

[2] M.P. Calvo and J.M. Sanz-Serna, Heterogeneous multiscale methods for mechanical systems with vibrations. *SIAM J. Sci. Comput.* **32** (2010) 2029–2046.

[3] P. Chartier, A. Murua and J.M. Sanz-Serna, Higher-order averaging, formal series and numerical integration I: B-series. *Found. Comput. Math.* **10** (2010) 695–727.

[4] Y.K. Chembo, L. Larger and P. Colet, Nonlinear dynamics and spectral stability of optoelectronic microwave oscillators. *IEEE J. Quant. Electron.* **44** (2008) 858–866.

[5] D. Cohen, E. Hairer and C. Lubich, Modulated Fourier expansions of highly oscillatory differential equations. *Found. Comput. Math.* **3** (2005) 327–450.

[6] M. Condon, A. Deaño and A. Iserles, On second order differential equations with highly oscillatory forcing terms. *Proc. Roy. Soc. A* **466** (2010) 1809–1828.

[7] M. Condon, A. Deaño and A. Iserles, On systems of differential equations with extrinsic oscillation. *Discrete Contin. Dyn. Syst.* **28** (2010) 1345–1367.

[8] B. Engquist, A. Fokas, E. Hairer and A. Iserles Eds., *Highly Oscillatory Problems*. Cambridge University Press, Cambridge, UK (2009).

[9] Y.N. Kyrychko and S.J. Hogan, On the use of delay equations in engineering applications. *J. Vibr. Control* **16** (2010) 943–960.

[10] V.S. Udaltsov, J.P. Goedgebuer, L. Larger, J.B. Cuenot, P. Levy and W.T. Rhodes, Cracking chaos-based encryption systems ruled by nonlinear time delay differential equations. *Phys. Lett. A* **308** (2003) 54–60.

[11] G.D. van Wiggeren and R. Roy, Communication with chaotic lasers. *Science* **279** (1998) 1198–1200.

[12] S. Wirkus and R. Rand, The dynamics of two coupled van der pol oscillators with delay coupling. *Nonlinear Dyn.* **30** (2002) 205–221.